Supramolecular Crosslinked Hydrogels: Similarities and Differences with Chemically Crosslinked Hydrogels

Sandrine Laquerbe, Julien Es Sayed, Cédric Lorthioir, Christophe Meyer, Testuharu Narita, Guylaine Ducouret, Patrick Perrin, Nicolas Sanson

Supramolecular Crosslinked Hydrogels: Similarities and Differences with Chemically Crosslinked Hydrogels

Sandrine Laquerbe, Julien Es Sayed, Cédric Lorthioir, Christophe Meyer, Tetsuharu Narita, Guylaine Ducouret, Patrick Perrin, Nicolas Sanson**

KEYWORDS. Hydrogel; supramolecular crosslinker; supramolecular chemistry; stimuli-responsive.

ABSTRACT

The specific design of a water-soluble supramolecular crosslinker based on a terpyridine-iron(II) bis-complex is reported. Copolymerization of this crosslinker with acrylamide monomers in water allows a novel one-step synthesis of metallo-supramolecular hydrogels. The synthesized hydrogels were characterized by rheology, dynamic light scattering and ^{1}H DQ NMR experiments. They reveal great similarities with the rheological behavior of a chemically crosslinked acrylamide network but differences in the structure at low length scales.

Characterization also shows that the supramolecular crosslinker behaves similarly to a permanent bond at the observed timescales (from 10^{-6} to almost 1000 s), thanks to its relatively high binding energy. However, unlike their chemical counterparts, supramolecular gels show a polyelectrolyte swelling behavior and a stimuli-responsiveness when put in contact with an oxidant. A controlled tuning of the physical-chemical properties of the final gel, ranging from the initial supramolecular gel properties to those of a polymer solution, is then achievable.

INTRODUCTION

Hydrogels are 3D networks of polymer chains that are connected to one-another via crosslinks and swollen in a large quantity of water. They have become very popular in various domains from biomedical applications (contact lenses, tissue engineering, drug delivery systems) to care products or agriculture.[1–3] Hydrogels are conventionally separated in two main classes: chemically- and physically- crosslinked networks. In the former case, polymer chains are interconnected by permanent covalent bonds, which make the gels unable to self-heal for instance. Their physical counterparts are based on specific and dynamic non-covalent crosslinks, thereby allowing stimuli-responsiveness and versatility.[4,5] Supramolecular chemistry offers numerous examples of such interactions which cover a wide range of binding strengths and dynamics. In aqueous media, this precious toolbox provides host-guest interactions, multivalent ionic interactions as well as hydrogen bonding or formation of stereocomplexes, to mention just a few. Among these interactions, metal-ligand complexation and, in particular, terpyridine complexes of transition metals, lanthanide or actinide cations are of great interest due to numerous advantages. As an example, one can mention their highly-directional interactions and high thermodynamic stability.[6,7] Depending on the metal ions, very different dynamics can be achieved thus offering a remarkable versatility to the system.[8,9] Potts et al. and Hanabusa et al.

were among the first to incorporate terpyridine groups in polymer chemistry by copolymerization of terpyridine-based monomers with various monomers like styrene, vinyl acetate, or acrylic acid.[10,11] Nowadays, such incorporation of terpyridine groups in macromolecular systems has become widespread and different architectures have been designed.[12,13] In particular, Tew et al. and Schubert et al. have shown that adding metal ions to a solution of polymers bearing terpyridine groups increases the viscosity reflecting the connection between the polymer chains.[14,15] This was the first report on metallo-supramolecular gels crosslinked through terpyridine-metal interactions. Then, similar systems were developed featuring variations of the polymer backbone (monomers nature and distribution) and of the metal cations. Nevertheless, all these studies focus on the synthesis of gels in organic solvents.

As regards hydrogels crosslinked with terpyridine-metal complexes, their preparation as reported in the literature consists in a complex and time-consuming two-step preparation method.[16–18] In a first step, a hydrophilic polymer bearing pendant hydrophobic terpyridine groups is synthesized in an organic solvent and transferred into water. Then a metal salt is added to form a physically crosslinked hydrogel by polymer association through the formation of terpyridine-metal complexes. For example, Brassine et al. synthesized a side-chain functionalized poly(2-(dimethylamino)ethyl methacrylate) by controlled radical copolymerization with terpyridine-modified methacrylate monomer in dioxane.[19] Then, a supramolecular hydrogel was obtained by solubilization of the synthesized polymer chains in an aqueous solution of cobalt(II) cations. However, Xu et al. and Asoh et al. pointed out that such a method may not be adapted to the preparation of hydrogels based on complexes with fast kinetics and high thermodynamic stability.[20,21] Indeed, in the case of ions like iron(II) or nickel(II), their strong binding energy with terpyridine ligands leads to a limited diffusion of

metal ions in the polymer network and favors the formation of intrachain rather than interchain crosslinks. As a result, heterogeneous network structures are formed with a significant fraction of non-elastically active chains, that decreases the elastic modulus of the gels. Ahmadi et al. observed similar results on networks build up from tetra-armed poly(ethylene glycol) (PEG) chains the free extremity of which are connected via click chemistry carry two terpyridine pendant groups.[22] Despite the controlled topology and the limited inhomogeneities of these chemically crosslinked networks, the addition of metal cations that interact strongly with terpyridines leads to the formation of numerous intrachain loops in addition to physical junctions between distinct network chains. In previous papers, this preparation method based on polymer association rather than polymerization offers a comprehensive model system for a deeper understanding of the impact of the supramolecular junction dynamics on the rheological and mechanical properties of the networks.[23,24] Metallo-supramolecular hydrogels were synthesized using a micellar copolymerization in water of a hydrophobic terpyridine-modified monomer and a hydrophilic acrylamide monomer.[25] Even though if the change of solvent is not needed in this case, a purification step is required to wash out the surfactant molecules before adding metal ions. In addition, this polymerization approach leads to polymer chains with hydrophobic blocks, the size of which is related to the number of hydrophobic monomers initially contained into the micelles.[26] In the light of reported studies, unlocking the limitations related to the two-step synthesis in different solvents appears challenging.

Within this scope, we report on a one-step synthesis of metallo-supramolecular hydrogels using a synthesized water-soluble supramolecular crosslinker based on a terpyridine-iron(II) bis-complex. First, the supramolecular crosslinker can directly copolymerize with hydrophilic monomers in water to form hydrogels that are efficiently crosslinked with terpyridine-metal

interactions displaying high-binding strength. We propose a comparative and intensive study between two polyacrylamide networks that are synthesized under similar conditions except that one involves physical crosslinks based on metallo-supramolecular interactions (called Supra-PAM) while the other is chemically crosslinked (called Chem-PAM). This study shows that the chosen strategy allows the preparation of supramolecular hydrogels with rheological properties comparable to those of covalently crosslinked ones but with a dormant ready-to-be-used responsive functionality. Indeed, the supramolecular crosslinker behaves similarly to a chemical crosslinker, which connects chains by permanent bonds, on the timescale probed by both rheology and dynamic light-scattering. The evolution of the network structure of both kinds of hydrogels, Supra-PAM and Chem-PAM, with the crosslinker amount was investigated by proton double-quantum (DQ) NMR. The obtained results showed that despite similar elastic moduli, the structure of both networks differs in terms of the distribution of the density of elastically effective chains and the overall fraction of repeat units that they involve. Another difference stands in the fact that the supramolecular hydrogels show a swelling behavior different from the one of Chem-PAM gels and are able to undergo a gel-to-sol transition when an external stimulus (chemical oxidant) is applied. This latter property underlines the ability of the supramolecular crosslinker to dissociate and re-associate reversibly, which allows the accurate tuning of the overall crosslinking density, and so, of the hydrogel macroscopic properties.

EXPERIMENTAL SECTION

Materials

All reagents were purchased from Sigma Aldrich and used without further purification unless otherwise indicated. 2-[2-(2-aminoethoxy)ethoxy]ethanol and 4'-chloro-2,2':6',2''-terpyridine

(Tpy-Cl) were purchased from ABCR and Fisher Scientific respectively. Anhydrous iron(II) chloride ($FeCl_2$, 99.5%) was also purchased from ABCR and stored under nitrogen (N_2) and dry conditions to prevent its oxidation by air. 2,2'-azobis[2-(2-imidazolin-2-yl)propane]dihydrochloride (VA044) was purchased from Wako. Ultrapure deionized water with a minimum resistivity of 18 MΩ.cm (milliQ, Millipore, France) was used for all experiments.

Synthesis

Compound 1. 2-[2-(2-aminoethoxy)ethoxy]ethanol (3.10 mL, 22.4 mmol, 1.2 eq) was added to a suspension of freshly finely ground potassium hydroxide (5.80 g, 104.0 mmol, 5.5 eq) in anhydrous DMSO (80 mL) under an argon atmosphere. After 1 h heating at 60 °C, Tpy-Cl (5.01 g, 18.7 mmol) was added and the resulting mixture was stirred at 60 °C. After 48 h, the reaction mixture was cooled to room temperature and poured into deionized water (800 mL). The resulting mixture was stirred and then left at rest for 3 h before being extracted with dichloromethane (CH_2Cl_2, 3 x 500 mL). The combined extracts were dried over $MgSO_4$ and then concentrated under reduced pressure. The residual DMSO was removed by heating the residue under reduced pressure (about 0.5 mmHg) at 80-90 °C. An orange-brown viscous liquid was obtained (4.91 g, yield = 69 %).

Half crosslinker 2. Compound **1** (4.91 g, 12.9 mmol) was dissolved in anhydrous tetrahydrofuran (70 mL). Triethylamine (2.20 mL, 15.7 mmol, 1.2 eq) and acryloyl chloride (1.20 mL, 14.8 mmol, 1.15 eq) were successively added dropwise at 0 °C. After 2 h stirring at room temperature, the reaction mixture was concentrated under reduced pressure. The residue was dissolved in CH_2Cl_2 (200 mL) and the resulting solution was washed with deionized water (2 x 50 mL) and a NaCl saturated solution (50 mL, prepared with deionized water). The organic

phase was dried over $MgSO_4$, filtered and concentrated under reduced pressure to give a brown solid residue which was triturated in diethyl ether (Et_2O, 50 mL). The resulting suspension was allowed to sediment and the supernatant was then removed using a syringe fitted with a needle. This operation was repeated twice and the suspension of the solid in Et_2O (50 mL) was eventually filtered through a fritted glass. The collected solid was dried under reduced pressure (0.5 mmHg) to obtain 3.33 g (yield = 59%) of **2** as a beige powder.[27] The stoichiometry between terpyridine and vinyl functions was confirmed by NMR. **^{1}H NMR** (400 MHz, $CDCl_3$, δ (ppm)) 8.67 (app br d, J = 5.0 Hz, 2H, Tpy), 8.61 (br d, J = 8.0 Hz, 2H, Tpy), 8.05 (s, 2H, Tpy), 7.86 (td, J = 7.8 and 1.8 Hz, 2H, Tpy), 7.34 (ddd, J = 7.4, 4.8 and 1.1 Hz, 2H, Tpy), 6.38 (br s, 1H, N**H**-C(O)-CH=CH_2), 6.24 (dd, J = 17.0 and 1.6 Hz, 1H, NH-C(O)-CH=C**H$_2$**), 6.09 (dd, J = 17.0 and 10.2 Hz, 1H, NH-C(O)-C**H**=CH_2), 5.55 (dd, J = 10.2 and 1.6 Hz, 1H, NH-C(O)-CH=C**H$_2$**), 4.42 (app t, J = 4.6 Hz, 2H, Tpy-O-C**H$_2$**-), 3.92 (app t, J = 4.6 Hz, 2H, Tpy-O-CH_2C**H$_2$**-), 3.73-3.52 (four m, 8H, -O-C**H$_2$**C**H$_2$**-), see Figure S1 for peak assignments. **^{13}C NMR** (100 MHz, $CDCl_3$, δ (ppm)) 167.1 (C, Tpy), 165.7 (NH-**C**=O), 156.9 (C, Tpy), 155.7 (C, Tpy), 148.9 (CH, Tpy), 137.2 (CH, Tpy), 131.0 (**C**H=CH_2), 126.4 (CH=**C**H_2), 124.1 (CH, Tpy), 121.6 (CH, Tpy), 107.7 (CH, Tpy), 71.0-70.4 (-O**C**H_2**C**H_2O-), 69.9 (-**C**H_2CH_2NH-), 69.6 (Tpy-OCH_2**C**H_2-), 68.0 (Tpy-O**C**H_2-), 39.4 (-**C**H_2NH-).

***Crosslinker 3*.** Compound **2** (0.101 g, 0.0232 mmol) was dissolved in methanol (MeOH, 10 mL) at about 35 °C under N_2 atmosphere. A 0.2 M stock solution of $FeCl_2$ was freshly prepared by dissolving 66.0 mg (0.49 mmol) of anhydrous $FeCl_2$ in MeOH (3 mL) and 1 mL of the resulting solution (0.71 eq) was added dropwise to solution of compound **2** under stirring. The solution turned to dark purple directly after the addition of the metal salt. After 2 h, the solvent was evaporated under a stream of N_2 and then under reduced pressure (10 mm Hg) leading to a

dark purple solid (0.126 g, yield ≈ 98%). **^{1}H NMR** (400 MHz, D_2O, δ (ppm)) 8.38 (s, 4H, Tpy), 8.27 (app br d, J = 8.0 Hz, 4H, Tpy), 7.68 (app t, J = 7.6 Hz, 4H, Tpy), 7.03 (br d, J = 5.2 Hz, 4H, Tpy), 6.89 (app t, J = 6.2 Hz, 4H, Tpy), 6.06 (dd, J = 16.8 and 10.4 Hz, 2H, NH-C(O)-CH=C**H$_2$**), 5.89 (d, J = 17.2 Hz, 2H, NH-C(O)-C**H**=CH_2), 5.40 (d, J = 10.4 Hz, 2H, NH-C(O)-CH=C**H$_2$**), 4.65 (app br s, Tpy-O-C**H$_2$**-), 4.04 (app br s, 4H, Tpy-O-CH_2C**H$_2$**-), 3.77-3.32 (four m, 16H, -O-C**H$_2$**C**H$_2$**-), see Figure S2 for peak assignments. **^{13}C NMR** (100 MHz, $CDCl_3$, δ (ppm)) 167.1 (C, Tpy), 165.7 (NH-**C**=O), 156.9 (C, Tpy), 155.7 (C, Tpy), 148.9 (CH, Tpy), 137.2 (CH, Tpy), 131.0 (**C**H=CH_2), 126.4 (CH=**C**H_2), 124.1 (CH, Tpy), 121.6 (CH, Tpy), 107.7 (CH, Tpy), 71.0-70.4 (-O**C**H_2**C**H_2O-), 69.9 (-**C**H_2CH_2NH-), 69.6 (CH2, Tpy-OCH_2**C**H_2-), 68.0 (Tpy-O**C**H_2-), 39.4 (-**C**H_2NH-). **UV-Vis** (Distilled water): λ_{max} (ε) = 556 nm (10.810 L.mol^{-1}.cm^{-1}).

***Hydrogel preparation*.** Acrylamide (AM) monomers and the crosslinker were dissolved into deionized water. *N*,*N*′-methylenebisacrylamide (MBA) and the supramolecular crosslinker **3** were respectively used for chemically- (Chem-PAM) and physically- (Supra-PAM) crosslinked hydrogels. After addition of a freshly prepared aqueous solution of VA044, the solution was stirred during a few seconds. In a glovebox, the reaction mixture was transferred into a mold consisting of two parallel glass slides covered with PET films and separated by a 1 mm-thick silicon gasket. The reactor was then hermetically locked up under N_2 atmosphere and kept at 30 °C in an oven. After 40 h, the hydrogel was taken out from the mold and cut into different shapes depending on the characterization experiments. The monomer concentration and the initiator-to-monomer ratio were respectively set at 8 wt% and 0.2 mol% for all synthesized samples and the crosslinking ratio (molar ratio of crosslinker to the AM monomers) varied from 0 to 0.4 mol%.

All the solutions were degassed by bubbling N_2 to prevent scavenging of free radicals by O_2 during polymerization.

Swelling experiments. Swelling experiments were performed on disks of hydrogels either in pure water or in aqueous KCl solutions (concentration ranging from 10^{-5} to 10^{-1} M) at 25 °C. At regular time intervals, samples were removed from the solution, weighted ($m_{gel}(t)$) and then swollen again onto a fresh solution. Such measurements were repeated until the weight of swollen gels was constant, i.e. until they reached the equilibrium swelling. At the end of the experiment, the samples were dried at 60 °C to constant weight (m_{dry}). For each concentration of KCl and for pure water, swelling measurements were performed on two samples of the same synthesized hydrogel, considered in the preparation state.

The weight ratio $Q_m(t)$ is determined using the following equation:

$$Q_m(t) = \frac{m_{gel}(t)}{m_{dry}}$$

in which $m_{gel}(t)$ and m_{dry} are the weight of gel at swelling time t and after drying the extracted gel respectively. The value of this weight ratio at equilibrium, i.e. the plateau value of $Q_m(t)$ will be denoted $Q_{m,eq}$ in the following.

Stimuli-responsive experiments. Potassium persulfate (KPS) was used as an oxidant to cleave the supramolecular hydrogel crosslinks. A uniaxial compression test was performed on weighted disks of freshly prepared hydrogels using a rheometer (10 μm.s^{-1}, 25 °C). Then, samples were immersed in a KPS solution ([KPS] = 5.10^{-3} M) at 25 °C. After a given time, KPS was washed out from the network by immersing the swollen disks in pure water that was frequently changed. Finally, the samples were characterized by uniaxial compression tests and UV-visible spectroscopy before being dried in order to determine their swelling ratio. This protocol was

repeated with different immersing time in KPS solution and different molar KPS/crosslinker ratio in order to achieve various final states of the gel.

Instrumentation

NMR Spectroscopy. NMR experiments were performed on a Bruker Avance III HD spectrometer operating at 400 MHz for ^{1}H and 100 MHz for ^{13}C, using a standard 5 mm broadband SmartProbe regulated at 25 °C and D_2O or $CDCl_3$ as solvent.^{1}H NMR data are reported as follows: chemical shift in ppm using the solvent signal as reference, multiplicity (with standard abbreviations: s = singlet, d = doublet, t = triplet, q = quartet, m = multiplet or overlap of non-equivalent resonances, app = apparent, br = broad), integration. ^{13}C NMR data are reported as follows: chemical shift in ppm using the solvent signal as reference ($CDCl_3$: δ = 77.16 ppm), carbon environment (deduced from DEPT and HSQC experiments).

Polymerization kinetics. During the gel formation, the polymerization kinetics were monitored by solution-state NMR through the disappearance of the contributions that correspond to the protons of the double bond of both AM monomers and unreacted crosslinker. The ^{1}H NMR experiments were performed on a Bruker Avance III 300 MHz NMR spectrometer equipped with a Bruker 5 mm z-gradient BBFO probe. For each polymerization kinetics, the optimization of the experimental conditions used to monitor the time evolution of the quantitative ^{1}H single-pulse NMR spectrum was carried out on the aqueous solution prior to the addition of the initiator. In particular, the determination of the ^{1}H 90° pulse length (10.3 μs) as well as the adjustment of the recycle delay were performed in this initial stage of the sample. The sealed NMR tube was then lifted out from the magnet, the required amount of initiator was added to the solution without opening the tube and the sample was quickly inserted back in the magnet. One scan was performed every 70 s over an experimental time of 8 h. The sample temperature was regulated to

30 °C, after a temperature calibration of the probe head using methanol. Then, the conversion was determined based on the following equation: $Conversion = 1 - \frac{I(CH_2,\ t)}{I(CH_2,\ 0)}$ in which $I(CH_2,\ t)$ denotes the area under the peak corresponding to the vinylic protons =CH_2 in the cis position compared to =CH at polymerization time t and $I(CH_2,\ 0)$ stands for the area under the same peak at initial time (just after addition of the initiator).

Proton double-quantum (DQ) solid-state NMR. The ^{1}H multiple-quantum NMR experiments were performed at room temperature, under static conditions, on a 300 MHz Bruker Avance III HD NMR spectrometer and a 7 mm ^{1}H-X double-resonance MAS probehead. The hydrogels were prepared within the rotors, with a sample volume restricted to the central part of the RF coil, but high enough to allow the ^{1}H NMR peaks of the polymer protons and the one resulting from the residual water protons to be well-resolved. The pulse sequence used is the one proposed by Baum and Pines,[28] later improved by Saalwächter.[29] The ^{1}H 90° pulse length was equal to 3.2 µs and the recycle delay, set to 2.5 s, was adjusted according to the $T_1(^1H)$ relaxation time determined for the protons from the polymer chains.

In these experiments, two separate signals are monitored as a function of the excitation time, t_{DQ}: the ^{1}H multiple-quantum build-up curve, mostly governed by the double-quantum coherences, $S_{DQ}(t_{DQ})$, and the reference signal, $S_{Ref}(t_{DQ})$. This latter is composed from the contributions from the 4n quantum orders, the dipolar-encoded longitudinal magnetization as well as the ones from protons of repeat units displaying isotropic reorientations. After subtraction of this last contribution from S_{Ref}, the ratio between S_{DQ} and the sum of S_{DQ} and the thus-corrected S_{Ref} signal leads to the normalized ^{1}H double-quantum build-up curve, $I_{DQ}(t_{DQ})$. The details of this data analysis is reported elsewhere.[29] In the present case, these experiments were performed at high NMR field, so that the curve $I_{DQ}(t_{DQ})$ related to the protons from the polymer

chains could be selectively determined. In this way, the fraction of elastically effective chains, f_{EEC}, within the hydrogels could be accurately derived.

The time-evolution of $I_{DQ}(t_{DQ})$ was used to determine the distribution, $P(D_{Res})$, of the residual ^1H-^1H dipolar coupling within the hydrogels, using the following expression:

$$I_{DQ}(t_{DQ}) = \int P(D_{Res}) \times i(D_{Res}, t_{DQ}).dD_{Res}$$

$i(D_{Res}, t_{DQ})$ corresponds to the expression of the normalized build-up curve for an elastically active chain related to a dipolar coupling equal to D_{Res}. $i(D_{Res}, t_{DQ})$ can be written as[30]:

$$i(D_{Res}, t_{DQ}) = \frac{1}{2}\left[1 - e^{-(0.378 \times D_{Res} \times t_{DQ})^{1.5}} \times \cos(0.583 \times D_{Res} \times t_{DQ})\right]$$

Since D_{Res} is proportional to the density of topological constraints (crosslinks or entanglements), the distribution $P(D_{Res})$ allows the heterogeneities in the polymer network topology within the hydrogels to be investigated.

UV-Visible Spectroscopy (UV-Vis). The optical absorbance measurements were carried out with a UV–Vis Hewlett-Packard 8453 spectrophotometer using a 1 cm path length quartz cell, in a wavelength range from 200 to 1100 nm and equipped with a temperature controller (± 0.1 °C). If not stated otherwise, temperature was set at 25 °C.

Measurements on hydrogels were also performed on the same instrument thanks to a specifically designed tank. Supramolecular gel samples were stuck on a quartz slide that was placed in the middle of the tank. The absorbance spectrum was measured in a wavelength range from 200 to 1100 nm. The gel thickness was measured by image analysis of side profile pictures of the samples. From this measurement and the absorbance at 556 nm, the supramolecular crosslinker concentration in the gel was calculated. As samples were larger than the light beam,

it was possible to perform other measurements at different positions of the gel on the quartz slide to evaluate the error on the crosslinker concentration.

Rheology. Small-strain oscillatory shear measurements were performed at 25 °C using a stress controlled TA Instruments DHR3 rheometer with parallel plates (plate diameter 20 mm). The top plate was chosen to be cross-hatched to prevent sample slipping. Hydrogels were cut into 22 mm-diameter disks using a stainless-steel punch. Normal force was set at 0.3 N to ensure the sample's contact with the top plate. The measured gap was around 1.5 mm. First, a short strain sweep (f = 1 Hz, γ = 0.1 % - 2 %) was performed to determine the linear viscoelastic regime. The strain sweep was stopped before the end of the viscoelastic plateau to preserve the sample. Then, a frequency sweep was carried out in the linear regime (γ = 1 %, ω = 0.01 rad/s - 100 rad/s) followed by a large strain sweep (f = 1 Hz, γ = 0.1 % - 100 %). To prevent solvent evaporation, the sample was fully immersed in paraffin oil. Comparison of the strain sweep experiments before and after adding oil showed that oil did not affect the viscoelastic properties on short timescales (a few hours). Besides, a time sweep experiment (γ = 1 %, ω = 1 rad/s) showed that the dynamic moduli recorded over several hours remained stable.

Uniaxial compression tests were performed on the same rheometer by using smooth parallel plates. A plate diameter of 20 mm was chosen so that the top plate was smaller than the sample diameter. Normal force was set at 0.1 N before applying a cycle of compression-tension at a constant rate (10 µm/s). The maximum deformation ranged from 15 % to 21 % depending on the sample. The compressional force and the gap were recorded during the test. From these data, the engineering stress σ and the deformation λ were determined by using the initial cross-sectional area of the sample and the initial gap. The Young modulus E was then determined from the slope of the linear curve $\sigma = f(\lambda - \lambda^{-2})$.

Dynamic Light Scattering (DLS). Dynamic light scattering measurements were performed with an ALV CGS-3 goniometry system (ALV, Langen, Germany), equipped with a cuvette rotation/translation unit (CRTU) and a He−Ne laser (22 mW at λ = 632.8 nm). This setup measures the time-averaged autocorrelation function of the scattered light intensity $g^{(2)}(t)$ at various scattering angles θ, i.e. at different values of the scattering vector q defined as $q = \frac{4\pi n}{\lambda} \sin\frac{\theta}{2}$, where n is the refractive index and λ is the laser wavelength (632.8 nm). As the supramolecular gel absorbs light at the laser wavelength, the scattered intensity I_{scatt} of all the studied gels is normalized by the intensity at 0 ° that is not absorbed by the gel:

$$\frac{I_{scatt}(\theta)}{I_0 10^{\varepsilon_{632.8\,nm}[supramolecular\ crosslinker]d}}$$

in which I_0 stands for the light intensity of the incident beam, $\varepsilon_{632.8\,nm}$ is the extinction coefficient of the supramolecular crosslinker at 632.8 nm ($\varepsilon_{632.8\,nm}$ = 948.3 $L.mol^{-1}.cm^{-1}$) and d is the inner tube diameter used to prepare the samples.

It was shown that hydrogels are non-ergodic systems since the time-averaged autocorrelation function is not equal to the ensemble-averaged one.[31] Indeed, crosslinks constrain the Brownian motion of polymer chains so that the average of concentration fluctuations does not equal to zero anywhere in the hydrogels but depends on the position. To overpass this difficulty, the sample was steadily vertically-translated during time-averaging so that the $g^{(2)}(t)$ function thus determined coincides with the ensemble-averaged correlation function (up to a cutoff delay time which mainly depends on the translation speed).

Hydrogels for DLS were directly prepared in 10 mm-diameter tubes using the same method than the one described above. All solutions were filtered using a syringe filter (0.45 µm, cellulose acetate membrane) prior to insertion in the tubes.

RESULTS AND DISCUSSION

Synthesis of supramolecular hydrogels

Supramolecular poly(acrylamide) hydrogels are elaborated by free-radical polymerization of acrylamide (AM) monomers in the presence of a new metallo-supramolecular crosslinker. This crosslinker **3**, corresponding to two terpyridine-functionalized monomers coordinated by iron(II), is designed in such a way that the reactive vinylic function has a chemical environment similar to that of the MBA chemical crosslinker. It is synthesized in three steps according to the protocol reported by Es Sayed et al. (Scheme 1 (a)). First, terpyridine groups were functionalized with a short ethylene oxide spacer capped on one end by an amine. Then, a terpyridine-based monomer **2** was formed by reaction with acryloyl chloride. Finally, the supramolecular crosslinker was formed by mixing the chemical reactant **2** in methanol with stoichiometric quantity of anhydrous $FeCl_2$ salt. The solution quickly turned to dark purple, indicating the formation of a terpyridine-based complex with iron(II), $[Fe(tpy)_2]^{2+}$, in methanol. As the bis-complex $[Fe(tpy)_2]^{2+}$ displays a characteristic metal-to-ligand charge transfer at 556 nm, the UV-visible spectroscopy allows the amount of incorporated crosslinker to be accurately quantified ($\varepsilon_{556\ nm}$ = 10.810 $L.mol^{-1}.cm^{-1}$) (Figure S3). The formation of the $[Fe(tpy)_2]^{2+}$ complex was also confirmed by ^1H NMR spectroscopy with a chemical shift variation for the protons of the terpyridine units (between 6.5 and 9.0 ppm)[32] (Figures S1 and S2). This result shows that the complexation was complete since the ^1H NMR peaks of free terpyridine are no longer detected on the spectrum of the crosslinker **3**. It was also observed that, due to the presence of charges, this supramolecular crosslinker is soluble in water which is one of the prerequisites to synthesize hydrogels in water.

Scheme 1. Procedure to prepare the supramolecular hydrogels: a) Route for the synthesis of the supramolecular crosslinker **3**; b) Method to prepare chemically- (Chem-PAM) (top) or physically- (Supra-PAM) (bottom) crosslinked hydrogels in aqueous media at T=30 °C.

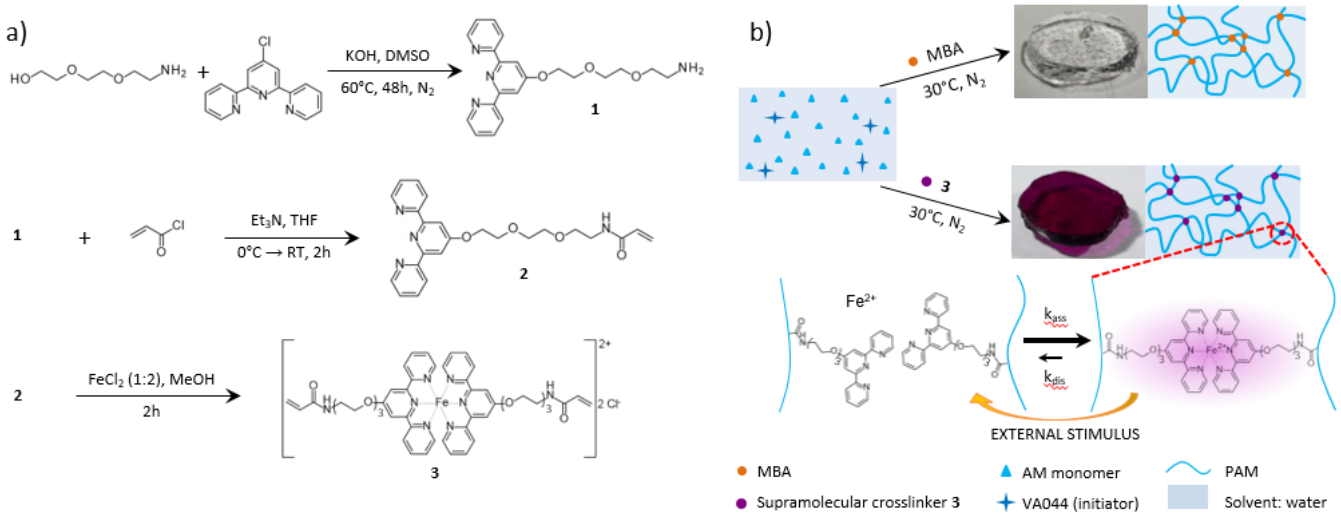

The copolymerization of AM and the designed supramolecular crosslinker **3** was thermally initiated at 30 °C and performed in water under inert atmosphere for 40 h to form a physically-crosslinked network. For comparison, a similar synthesis protocol was used with MBA to elaborate chemical gels. As shown in Scheme 1 (b), the synthesized hydrogels are transparent and homogeneous at the macroscopic length scale. Contrary to their chemical counterpart, the physically-crosslinked hydrogels are purple due to the presence of the supramolecular crosslinker based on terpyridine-iron(II) complexes, $[Fe(tpy)_2]^{2+}$.

A monitoring of polymerization kinetics by solution NMR showed that complete transformation of monomer and crosslinker double-bonds was achieved in approximatively 500 min at 30 °C for both kinds of gels (Chem-PAM and Supra-PAM, see Figure S4). Note that the complex involved in the synthesized supramolecular crosslinker remains stable during at least 780 min at 30 °C (Figure S5) meaning that its structure does not change over the polymerization.

In addition, since the thermodynamic constant of $[Fe(tpy)_2]^{2+}$ formation from each neat component (free terpyridines and free iron(II) cations) is estimated to $\beta_2 = 10^{20.9}$ $L^2.mol^{-2}$,[33] the chemical equilibrium is well shifted toward the complex formation. Such a high thermodynamic stability of the metallo-supramolecular complex ensures that the supramolecular crosslinker **3** species are all incorporated under their complexed form.

Structure-property relationship of hydrogels

The gel formation was confirmed by oscillatory rheology (Figure 1a). Indeed, supramolecular and chemical gels prepared with a crosslinker feed ratio of 0.1 mol% exhibit the rheological behavior expected for a viscoelastic solid. The strain sweep in Figure 1a displays a plateau of storage and loss moduli at low strain (up to about 20% of the strain amplitude), thus defining the linear viscoelastic regime. In this regime, the storage modulus is higher than the loss modulus (more than one order of magnitude), meaning that elasticity dominates the rheological behavior of both kinds of gels. As shown in Figure 1a, a similar storage modulus is achieved for both the chemically- (G' = 2500 Pa) and physically- (G' = 2600 Pa) crosslinked hydrogels.

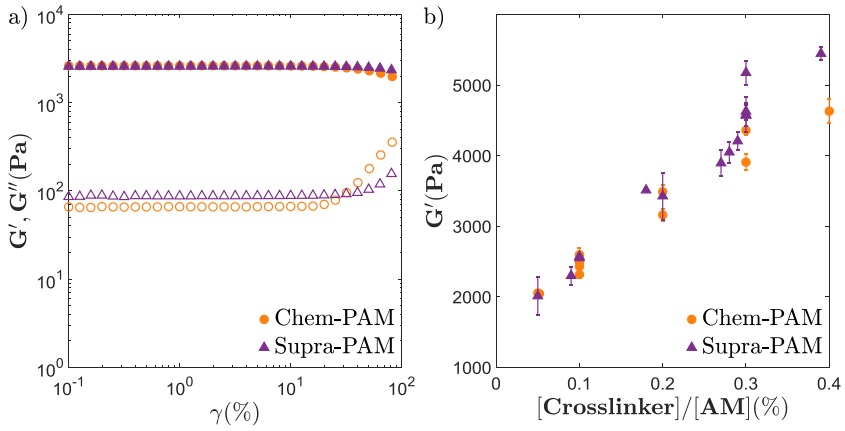

Figure 1. Dynamic shear properties of chemical (●) and physical (▲) hydrogels in their preparation state. a) Storage modulus (G', solid symbols) and loss modulus (G'', open symbols)

as a function of the strain amplitude (25 °C, f = 1 Hz) for both kinds of hydrogels (0.1 mol% of crosslinker). b) Storage modulus at f = 1 Hz and γ = 1 % for both kinds of hydrogels as a function of the crosslinker feed ratio.

When varying the crosslinker feed ratio, similar elasticity between chemically- and physically-crosslinked hydrogels is also observed (Figure 1b). For both kinds of gels, the storage modulus increases monotonically with the crosslinker feed ratio. On the basis of the theory of rubber elasticity, G' can be related to the molar concentration of elastically effective network strands, ν_{eff} (mol.m^{-3}), using the phantom network hypothesis:

$$G' = \left(1 - \frac{2}{f}\right) RT\nu_{eff} \quad (1)$$

Where f is the crosslinker functionality (equal to four for both kinds of polymer networks), R is the universal gas constant, T is the absolute temperature.[16,34]

Considering an ideal case in which all the incorporated crosslinker molecules connect elastically effective polymer chains build from the entire initial quantity of monomers, one can estimate ν_{eff} from the crosslinker feed ratio:

$$\nu_{eff} = \frac{2\,\phi}{M_{AM} v_{spe}^{pol}} . \frac{[Crosslinker]}{[AM]} \qquad (2)$$

Where M_{AM} is the monomer molar mass (71.08 g.mol^{-1}), ϕ is the polymer volume fraction, and v_{spe}^{pol} is the specific volume of the polymer (0.741 cm^3.g^{-1}).

Finally, the estimated value of the elastic modulus derived from eqs (1) and (2) is larger than the experimental one for both kinds of gels and for all crosslinker concentrations, except 0.05 mol% (Table S1). Such a difference with the theoretical value, that was also observed in the literature for Chem-PAM networks, is explained by the formation of network topological defects like dangling chains or loops and by the presence of significant heterogeneities of the gel crosslink density.[35–37] Indeed, it was reported that the structure of a poly(acrylamide) network

crosslinked with MBA is characterized by the presence of crosslinker-rich clusters surrounded by regions composed of long, weakly crosslinked polymer chains.[35,37–41] Weiss et al. suggested that each cluster could act as a single effective crosslink, therefore decreasing the apparent concentration of crosslinking agent.[38] Thus, the similar values of the elastic modulus measured for both Chem-PAM and Supra-PAM hydrogels raise the question of the existence of a similar structure with crosslinker-rich clusters for the Supra-PAM networks.

Further understanding of the obtained network structures is then required and could be achieved through light scattering and proton double-quantum (DQ) NMR experiments, both techniques allowing to study hydrogels at different length scales. First, the normalized average scattered light intensities at 90 ° are $1.92.10^{-4}$ and $2.60.10^{-4}$ a.u. for the Chem-PAM gel and the Supra-PAM gel, both prepared with a crosslinker feed ratio of 0.1 mol%, respectively. This similarity in terms of the scattered light intensity reveals that the Chem-PAM and Supra-PAM gels show similar heterogeneities at the length scale probed by light scattering (40 – 200 nm). However, according to Gombert et al., the cluster size of chemically-crosslinked PAM networks for hydrogels prepared at similar crosslinker feed ratios is smaller than the length scale investigated by light scattering.[40] As a consequence, another technique is required to study the structure of Chem-PAM and Supra-PAM networks at the polymer chain level.

^{1}H DQ NMR experiments were performed on both kinds of hydrogels at different crosslinker feed ratios. Such measurements allow to probe their structure at shorter length scales than the one covered by light scattering. Indeed, this technique measures the residual proton-proton dipolar couplings, D_{res}, related to the elastically effective polymer chains. Due to crosslinks or entanglements at the extremities of these strands, the chain segments display anisotropic re-orientational motions over the tens of microseconds timescale, leading to a non-zero partial

motional averaging of the ^{1}H-^{1}H dipolar couplings. The higher the molecular weight M_x of a given elastically effective chain, the weaker the anisotropy and the lower D_{res}. As a result, the ^{1}H DQ NMR experiments provide a quantitative description of the network topology with two key parameters: the D_{res} distribution within the gels, $P(D_{res})$, related to the M_x distribution and the fraction of repeat units involved in the elastically effective chains, f_{EEC}.

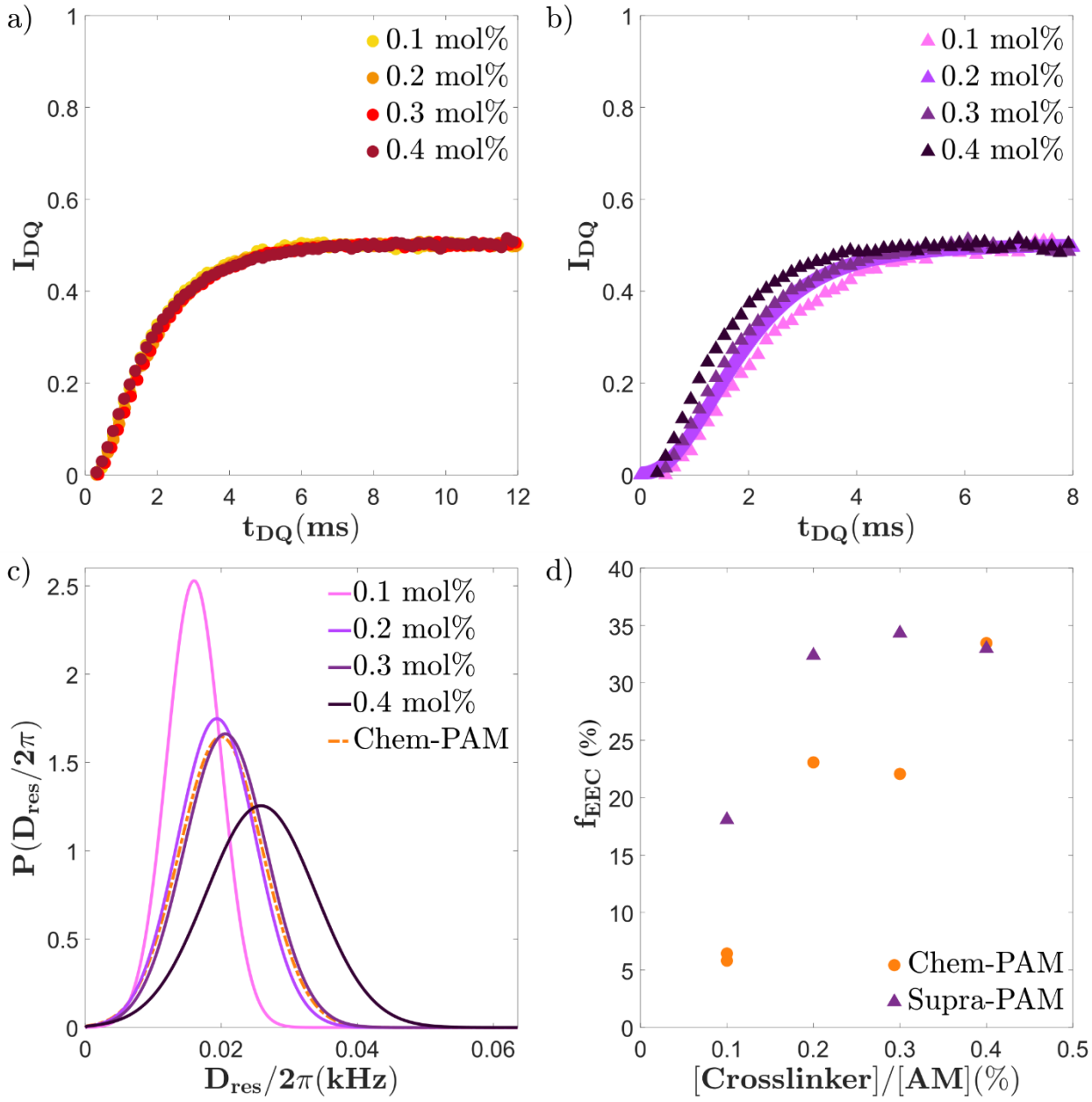

Figure 2. Normalized ^{1}H DQ intensity, I_{DQ}, as a function of the DQ excitation time, t_{DQ}, for (a) Chem-PAM and (b) Supra-PAM gels with different crosslinker to monomers ratios. (c) Distributions of D_{res}, $P(D_{res}/2\pi)$, deduced from the fit of the data reported in (a) and (b) using a Gaussian distribution. (d) Evolution of the fraction of the repeat units involved in elastically effective polymer chains, f_{EEC}, with the crosslinker feed ratio for Chem-PAM and Supra-PAM hydrogels.

First, the analysis of the ^{1}H DQ NMR signals reveals that the proportion of repeat units that are involved in elastically effective chains, f_{EEC}, is lower than 35 % for both chemical and supramolecular hydrogels (Figure 2d). Thus, more than 65 % of the polymer chain segments belongs to defects (dangling or free chains) that do not contribute to the elasticity of the hydrogel. Similar results were obtained by Zou et al. on chemically-crosslinked networks of acrylamide and acrylic acid.[42] It partially explains the deviations between the experimental and the theoretical values of elasticity measured on the Chem-PAM and Supra-PAM networks (Table S1). In the light of these results, equation (2) might be modified to estimate the molar concentration of elastically effective strands while taking into account the quantity of monomers that does not integrate the elastic network:

$$\nu_{eff} = \frac{f_{EEC}\,\phi}{v_{spe}^{pol} M_x} \qquad (3)$$

Figure 2d shows that f_{EEC} is mostly higher for the Supra-PAM gels than for the Chem-PAM gels and that it tends to increase with the crosslinker feed ratio. In other words, Supra-PAM gels exhibit a lower fraction of unit repeats in the network defects than Chem-PAM gels and this fraction decreases as the crosslinking agent concentration increases in both gels. This latter result is consistent with the elastic modulus increase observed in Figure 1b.

Focusing on the Chem-PAM gels, the normalized DQ build-up curves perfectly superimpose independently of the crosslinker feed ratio and f_{EEC} (Figure 2a). These $I_{DQ}(t_{DQ})$ data may be successfully described using a Gaussian distribution of D_{res}. As depicted in Figure 2c, the elastic network of all the Chem-PAM hydrogels can be represented by a unique and broad D_{res} distribution with median value of 125 Hz and a standard deviation equal to 39 Hz. Thus, although the crosslinking ratio is increasing, the mass distribution of polymer chains between two consecutive topological constraints is constant and therefore the topology of the Chem-PAM networks remains unchanged. As a result, more and more repeat units are involved in the elastically effective network that is growing by replication of its structure in a self-similar way. Since Chem-PAM gels are known to form structural heterogeneities with densely and poorly crosslinked regions,[35,37–40] one may consider that the concentration of elastically effective polymer chains is higher in the densely crosslinked regions. Thus, the measured mass distribution of polymer chains between crosslinks or entanglements should be dominated by the contribution from the network strands located in the clusters. The fraction of repeat units for the longer chains connecting clusters may be comparatively weaker and besides, the corresponding D_{res} values should be significantly lower so that the evolution of their contribution to $I_{DQ}(t_{DQ})$ with the crosslinking ratio may be difficult to detect.

A different behavior is clearly observed for the Supra-PAM gels. The growth rate of $I_{DQ}(t_{DQ})$ for the Supra-PAM samples remains lower than the ones for the Chem-PAM gels, up to a crosslinking ratio equal to 0.3 mol% at which the $I_{DQ}(t_{DQ})$ curves for both gels are similar (Figure 2b). This feature is equivalently detected by considering the evolution of the distribution of D_{res}, , with the supramolecular crosslinker concentration: below 0.3 mol%, the distribution $P(D_{res})$ shifts towards higher D_{res} values and gets broader, thus resulting to a similar distribution to the

one detected for Chem-PAM gels at 0.3 mol% of crosslinking agent (Figure 2c). The first conclusion that can be drawn from the DQ NMR results is that, at a given crosslinking ratio, both kinds of gels do not display the same structure at the macromolecular length scale. Below a crosslinking ratio of 0.3 mol%, Supra-PAM gels feature a rather homogeneous network with a higher proportion of longer elastically effective chains than the one in the Chem-PAM gels. At 0.3 mol% of crosslinker, both gels are characterized by the same mass distribution of network strands at the nanometric length scale but a different defect quantity (Figure 2d). At this stage, it is interesting to note that the evolution of the supramolecular gel structure with the crosslinker feed ratio is somewhat typical of rather homogeneous networks: the higher the number of crosslinking junctions, the shorter the network strands.

Finally, it is important to notice that the $I_{DQ}(t_{DQ})$ curves of Chem-PAM and Supra-PAM gels feature a plateau at 0.5 up to at least t_{DQ} = 8 ms. This result is expected for chemical gels but not necessarily for transient networks like supramolecular gels. This plateau implies that the end-to-end vector of the elastically effective chains does not undergo significant reorientations over this timescale. Therefore, such a behavior suggests that the supramolecular crosslinker and the entanglements act as permanent crosslinkers on the millisecond timescale.

In summary, the ^{1}H DQ NMR results evidenced that the supramolecular and the chemical gels feature a different distribution their elastically active polymer chains despite their similar rheological behavior in the linear viscoelastic domain. It also reveals a high stability of the supramolecular crosslinker over a few milliseconds. As a matter of fact, by definition, the lifetime of the supramolecular crosslinker is finite unlike MBA. In this respect, some differences in the junction dynamics between both Chem-PAM and Supra-PAM gels might be expected over a longer timescale. Further understanding of the physical gel dynamics compared to the chemical

ones is then required to assess how the designed crosslinker could impact the overall network properties.

Dynamics of supramolecular hydrogels

Small-amplitude oscillatory shear measurements and dynamic light scattering experiments were used to investigate the dynamics of the synthesized hydrogels. As shown in Figure 3a, the dynamic viscoelastic properties of both Chem-PAM and Supra-PAM hydrogels are characterized by a storage modulus value independent of the oscillation frequency and which is well-known as the rubbery elastic plateau. This latter is related to the restriction of polymer chain diffusive motions due to the junctions between these chains, such as entanglements (the effect of which occurs in the high-frequency regime) or crosslinks (in the low frequency regime).

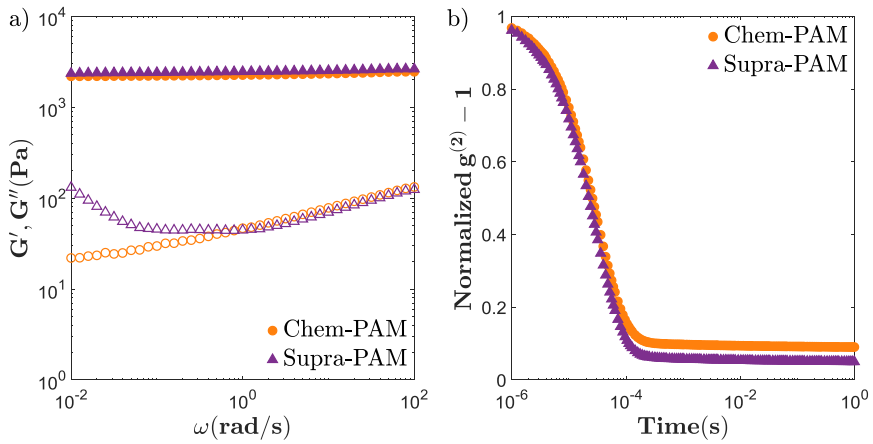

Figure 3. Comparison of Chem-PAM (●) and Supra-PAM (▲) hydrogels (0.1 mol% of crosslinker) in the preparation state. a) Storage modulus (*G'*, solid symbols) and loss modulus (*G''*, open symbols) as a function of the angular frequency (25 °C, γ = 1%) measured by rheology b) Normalized autocorrelation function $g^{(2)}(t)$-1 measured by DLS (25 °C; diffusion angle: 90 °).

One can notice the absence of cross-over between *G'* and *G''*, even in the low-frequency regime. As expected, the moduli cross-over, which represents the boundary between free-flowing and solid-like regimes, is not reached for chemically-crosslinked gels.[35,43] However, such a cross-over has already been observed in the case of metallo-supramolecular gels: its occurrence depends on the metal cation nature involved in the terpyridine bis-complex.[19,23] The cross-over is related to the ability of polymer strands to dissociate from their binding sites (transient crosslinking) and relax constraints. In a supramolecular network, the dynamics of such events is governed by two characteristic times: the relaxation time of the polymer strands, measured in the absence of crosslinking, and the lifetime of the transient crosslinks, which depends on the cation nature.[4,23,24,44] In our case, the relaxation time evaluated on solutions of linear PAM prepared in the same conditions as hydrogels (without crosslinker) is $\tau_{rept} \sim 10^2\ s$ (see Figure S6). As no relaxation is visible for the Supra-PAM hydrogels, the dynamics of the supramolecular hydrogels should be mainly governed by the lifetime of the terpyridine bis-complexes which should occur at a longer timescale.

To probe assess this hypothesis, dynamic light scattering measurements were performed to probe timescales (10^{-6} – 1 s) which are complementary to the dynamic range investigated by rheology (0.01 s – 100 s). Experiments were performed on both Chem-PAM and Supra-PAM hydrogels and the intensity autocorrelation function $g^{(2)}(t)$-1 was analyzed to get information on the dynamics of hydrogels. This analysis is more complex for gels than for polymer solutions because of their non-ergodic nature. For gels as for polymer solutions, light is scattered by the concentration fluctuations resulting from the thermally-activated motions of the polymer chains. However, contrary to dilute polymer solutions, the strands of a gel are not totally free to move as they are constrained by nearly-immobile crosslinks or entanglements. Thus, the concentration

fluctuations vary spatially and the autocorrelation function provides information on both the dynamic and static concentration gradients.[45]

In Figure 3b, the normalized $g^{(2)}(t)$-1 function measured for Chem-PAM (0.1 mol% of crosslinker) shows the typical dynamics of a chemical gel: it indeed exhibits a decay at around 10^{-4} s followed by a plateau. The characteristic time of this decorrelation mode, determined by fitting the field autocorrelation function using a stretched exponential function (no data shown), was found to be proportional to q^{-2}. Thus the decorrelation can be attributed to the so-called gel mode, which corresponds to the network strand fluctuations resulting from thermal agitation. The plateau value observed on Figure 3b corresponds to the non-fluctuating scattered light intensity due to the "frozen" structure of the gel, that is to say, the spatial heterogeneities blocked by the crosslinks that do not relax with time.

Interestingly, the normalized $g^{(2)}(t)$-1 functions determined for the Supra-PAM gels displays the same behavior. This similarity of the gel mode characteristic time suggests that the concentration fluctuations for both kinds of gels are similar. Besides, no other relaxation mode was observed over the studied time range. Indeed, in the case of some non-permanently crosslinked networks, a second decorrelation was observed due to the dissociation of the transient crosslinking junctions.[22,46] The absence of such a decorrelation process proves that the dynamics involved by the supramolecular crosslinker **3** is much slower than the observation timescale. In this respect, one can conclude that the Supra-PAM gels behave similarly to the Chem-PAM gels and their dynamics could be probed over a timescale larger than the one covered by DLS measurements (10^{-6} – 1 s). Hogg et al. and later Henderson et al. deeply studied the dynamics of terpyridine-based bis-complexes. They found that the dissociation kinetic constant of $[Fe(tpy)_2]^{2+}$ in water at 25 °C is extremely low: $k_{diss} = 1{,}6.10^{-7}$ s^{-1}.[9,47] The bis-

complex is hence kinetically stable and the lifetime of the supramolecular association is longer than the observation timescale of most experimental approaches. The stability of the designed supramolecular crosslinker allows the stability of the properties of the resulting supramolecular networks on large timescales (beyond 100 s typically).

Swelling properties of the supramolecular hydrogels

Despite similarities between both kinds of polymer hydrogels, the supramolecular crosslinked hydrogels exhibit a swelling behavior, either in pure water or in salt solution, different from that of the chemical ones, as shown in Figure 4.

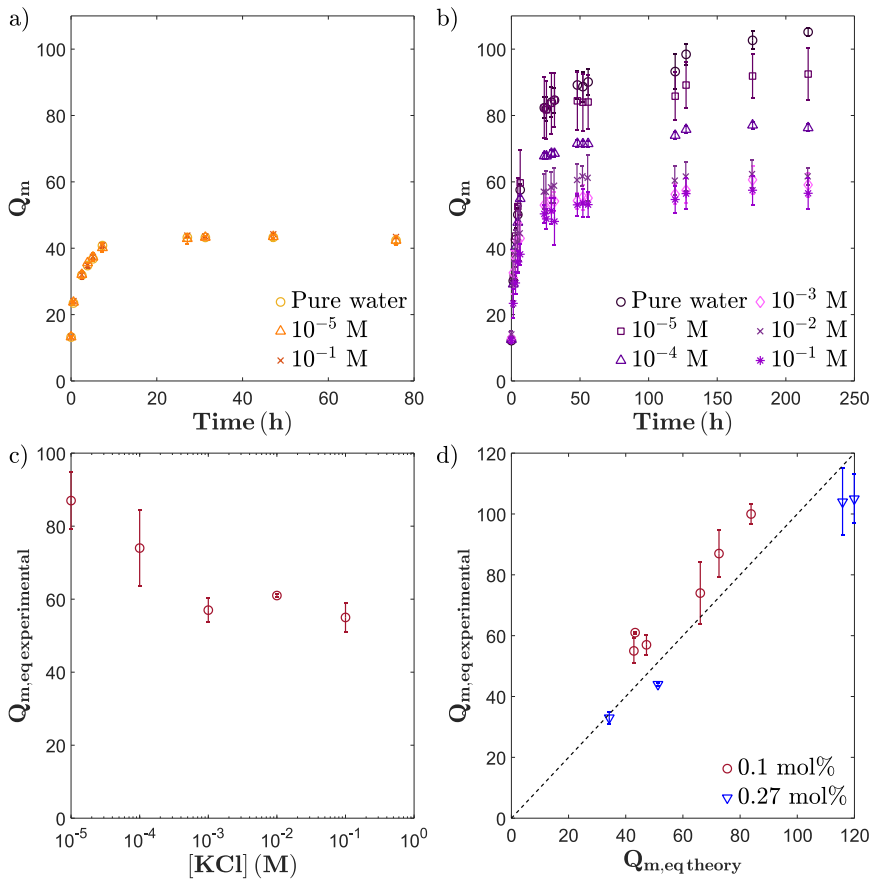

Figure 4. Swelling behavior of (a) chemical, Chem-PAM, and (b) physical, Supra-PAM, hydrogels (with a crosslinker feed ratio of 0.1 mol%) in pure water and in salt solution (KCl). Q_m denotes the mass swelling ratio-at 25 °C. The salt concentration was varied from 10^{-5} to 10^{-1} M. (c) Evolution of the swelling ratio at equilibrium with the KCl concentration for Supra-PAM gels prepared with 0.1 mol% of crosslinker. (d) Comparison of experimental and theoretical equilibrium swelling ratios for Supra-PAM gels, at different crosslinker concentrations. The theoretical data are computed using the Flory-Rehner and the ideal Donnan equilibrium models with $\chi_{12} = 0.47$.

On the one hand, the Chem-PAM network formed with 0.1 mol% of MBA exhibits a linear increase of the swelling ratio, $Q_m(t)$, with the square root of time up to an equilibrium plateau at $Q_{m,eq} = 43$ (Figure 4a). Besides, one can notice that their swelling behavior is not affected by the

presence of salt, irrespective of its concentration. The results are consistent with those reported in the literature for chemically-crosslinked PAM hydrogels and more generally, with the behavior theoretically expected for neutral gels.[37,48,49]

On the other hand, in pure water, the Supra-PAM hydrogel prepared with 0.1 mol% of crosslinker exhibits a larger equilibrium swelling ratio value ($Q_{m,eq}$ = 100) compared to the one of the Chem-PAM gel ($Q_{m,eq}$ = 43) (Figure 4b). In addition, the swelling ratio at equilibrium decreases from 100 to 52 as the salt (KCl) concentration is raised up to 10^{-1} M (Figure 4c). Such a behavior, typical of polyelectrolyte gels,[48,50] is not observed for the Chem-PAM gels, as expected. The polyelectrolyte behavior of the Supra-PAM gels is due to the nature of the supramolecular crosslinker, $[Fe(tpy)_2]^{2+}$, which indeed bears two positive charges (Scheme 1).[13] Besides, calculations of the swelling ratio at equilibrium for polyelectrolyte gels confirm that the Supra-PAM systems exhibit swelling properties typical of electrostatically-charged polymer networks (Figure 4d). Theoretical values are obtained by applying the Flory-Rehner model to both kinds of gels.[51] For neutral gels, the swelling equilibrium is determined by the competition between osmotic and elastic pressures as follows:

$$\Pi_m + \Pi_{el} = 0 \qquad (4)$$

$$\Pi_m = -\frac{RT}{V_1}\left(Ln(1-\phi) + \phi + \chi_{12}\phi^2 \right) \qquad (5)$$

$$\Pi_{el} = -\left(1 - \frac{2}{f}\right)\frac{RT}{v_{spe}^{pol} M_x}\, \phi_0{}^{\frac{2}{3}} \phi^{\frac{1}{3}} \qquad (6)$$

With *R,* the gas constant; *T,* the absolute temperature; V_1, the molar volume of the solvent (18.10^{-6} $m^3.mol^{-1}$); ϕ, the polymer volume fraction in the swollen state; χ_{12}, the Flory-Huggins parameter that characterizes the polymer-solvent interactions; ϕ_0, the polymer volume fraction in the preparation state; v_{spe}^{pol} , the specific volume of the polymer (0.741 $cm^3.g^{-1}$); M_x, the molar mass of the strands between two consecutive crosslinks or entanglements and f, the crosslinker

functionality (equal to four for both chemical and supramolecular crosslinkers considered in the present study). For polyelectrolyte gels, the osmotic pressure of mobile counterions and the presence of salt in the immersing solution need to be taken into account using the Donnan equilibrium model:

$$\Pi_m + \Pi_{el} = \Pi_{ion}^{ext} - \Pi_{ion}^{gel} = -\Delta\Pi_{ion} \qquad (7)$$

$$\Delta\Pi_{ion} = RT\left(\sqrt{\left(\frac{\alpha\phi}{v_{spe}^{pol}M_{AM}}\right)^2 + 4{C_{salt}^{ext}}^2} - 2C_{salt}^{ext}\right) \qquad (8)$$

With α, the polymer ionization degree which is here determined by the crosslinker molar ratio; M_{AM}, the monomer molar mass and C_{salt}^{ext}, the salt concentration of the immersing solution. By using these equations without any adjustable parameter except χ_{12} and ϕ, one can evaluate the Flory-Huggins parameter, χ_{12}, using the chemical gel data. A value of 0.47 is found for χ_{12} at 25°C. Then, the values of the equilibrium swelling ratio for the supramolecular gels are computed, assuming that χ_{12} is not modified by the change in the nature of the crosslinker. Finally, Figure 4d shows a good agreement between theoretical and experimental values of the equilibrium swelling ratio for the Supra-PAM gels prepared with a crosslinker feed ratio of 0.27 and 0.10 mol%.

Stimuli-responsiveness of the supramolecular hydrogels

Differences between chemically- and physically- crosslinked networks extend beyond their local structure and their swelling behavior. Unlike chemical gels, the supramolecular hydrogels can indeed be activated by an external stimulus, meaning that the bis-complex between terpyridine groups and metal ions can possibly be disrupted so as to prompt the gel-to-sol

transition. In the literature, a competitive ligand,[15] pH[52] or an oxidant[53,54] were used to disrupt the bis-complex to make supramolecular gels lose their macroscopic properties.

In the present work, the Supra-PAM gel structure was suppressed by adding potassium persulfate (KPS) as an oxidizing agent. First, as a proof-of-concept, a few microliters of an aqueous KPS solution (40 molar equivalents of KPS with respect to the crosslinker) were added to a Supra-PAM gel prepared with a crosslinker concentration of 0.3 mol%. After 48 hours, the sample flows like a liquid and has turned from dark purple to yellow color (see Figure S7) showing that the gel can indeed be transformed into a polymer solution at a macroscopic level. By UV-Visible spectroscopy, the analysis of the polymer solution evidences the disappearance of the absorption band at 556 nm related to the $[Fe(tpy)_2]^{2+}$ bis-complex (see Figure S8). The same KPS treatment was applied to the Chem-PAM gels which did not exhibit any change of their macroscopic properties (see Figure S7).

Targeting a desired mechanical resistance of a Supra-PAM gel can *a priori* be achieved by performing a partial cleavage. The disruption of the terpyridine-metal cation bis-complexes and consequently the destructuration of the hydrogels depend on both the oxidant quantity and contact time with the oxidant. In order to investigate these key parameters, cleavage experiments were carried out by immersing Supra-PAM hydrogels crosslinked at 0.3 mol% in KPS solutions. The immersing time and the amount of KPS were varied to control the network structure breaking and to finely monitor the evolution of the rheological properties of the gels. To quench the effect of KPS at chosen immersion times, samples were consecutively immersed in pure water. The macroscopic evolution of the Supra-PAM gels as well as the rheological and UV-visible measurements are gathered in Figure 5. These measurements are normalized by the value obtained on samples immersed into pure water.

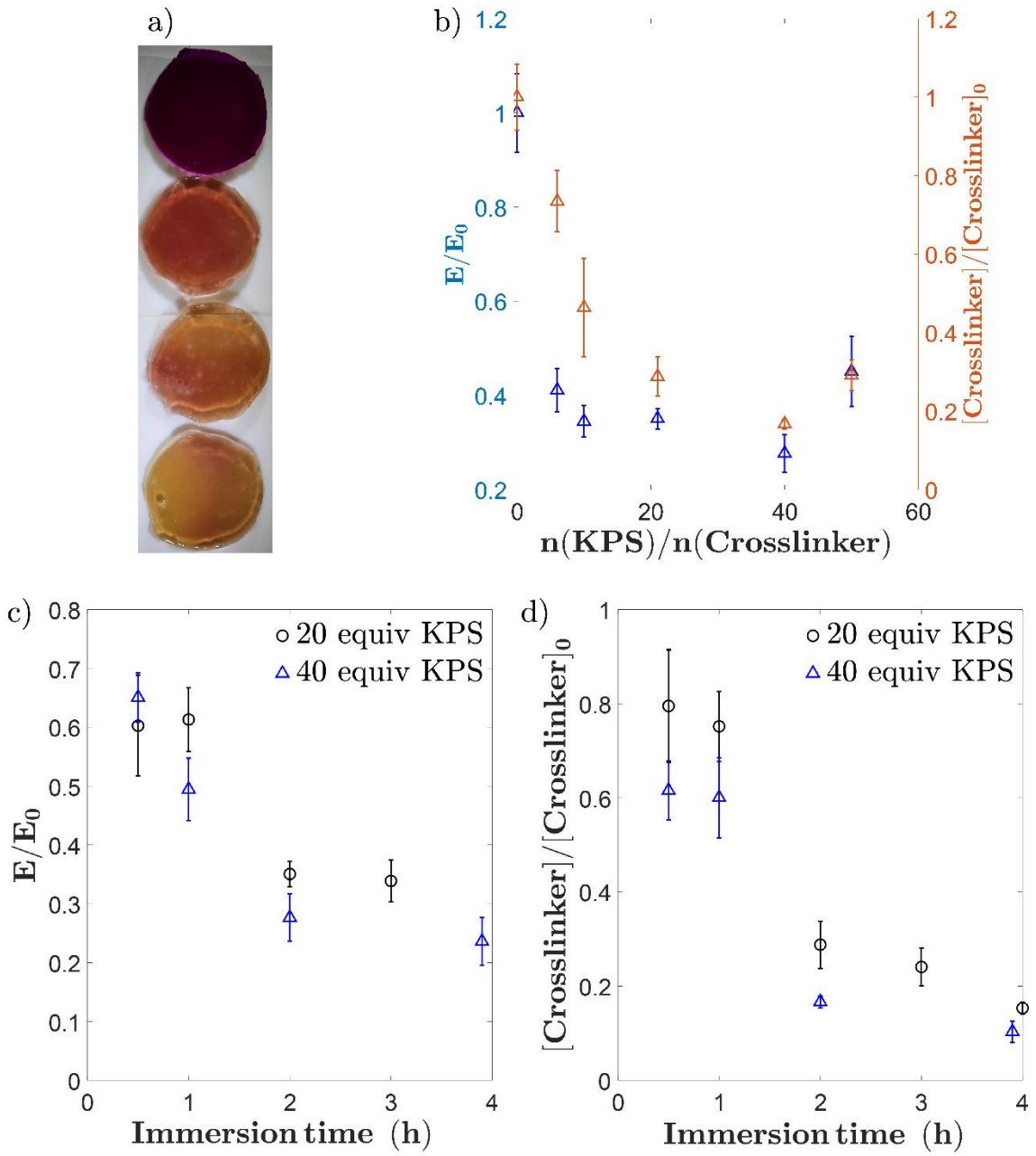

Figure 5. Partial cleavage of Supra-PAM gels (crosslinker feed ratio of 0.3 mol%) treated with KPS. (a) Visual aspect of samples immersed in a KPS solution during 3.5 h: the KPS quantity used increases from top to bottom (0, 10, 20 and 50 molar equivalents (equiv) compared to the crosslinker). (b) Evolution of the elastic modulus (blue) and supramolecular crosslinker

concentration in the gel (orange) with the relative quantity of KPS compared to the crosslinker (immersion time = 2 h). (c) Evolution of the Young modulus and (d) supramolecular crosslinker concentration in the gel as a function of the immersion time into the KPS solution (for 20 and 40 equiv KPS). All the measured data are normalized by the value obtained on the gel in the absence of KPS (E_0 ou $[Crosslinker]_0$).

The images of Supra-PAM gels immersed for te same duration in KPS solutions with different quantities of oxidizing agent (Figure 5a) show that their color gradually turns from purple to yellow, indicating the disappearance of the $[Fe(tpy)_2]^{2+}$ bis-complex in the network. Remarkably, the method allows the final crosslinker concentration to be varied while keeping a gel, as the broken structure does not flow. The rheological measurements reported on Figure S9 confirm this macroscopic observation. For all the samples, G' stands one to two orders of magnitude above G''. However, the gel mechanical properties are significantly modified by the oxidizing treatment. Figure b shows that the value of the elastic modulus of the Supra-PAM gels after immersion into the KPS solution for 3.5 hours is 70 to 80% lower than the one of the same gel swollen in pure water. The reduction of the elastic modulus increases with the KPS content, as expected, to reach a plateau value at 0.3. This non-linearity of the dependence of the elastic modulus upon the KPS concentration highlights the complexity of the phenomena involved including diffusion mechanisms of KPS in the network but also swelling and oxidation kinetics of Fe(II). UV-visible spectroscopy experiments carried out on the oxidized gels allow the $[Fe(tpy)_2]^{2+}$ complex concentration to be determined: this latter decreases while increasing the KPS content, for a given immersion time (Figure b), in agreement with the visual observations (Figure a). Similar measurements were performed while varying the immersion time into the KPS solution for a given quantity of KPS (Figure c and 5d). The results show that the bis-

complex concentration in the Supra-PAM gels decreases upon increasing the immersion time. The results reveal the versatility of the synthesized Supra-PAM gels that can be stimulated up to the formation of a solution or cleaved partially to get gels with given extent of crosslinking.

CONCLUSION

In the present work, we have reported the synthesis of a novel metallo-supramolecular crosslinker based on a high-binding strength terpyridine-iron(II) bis-complex, $[Fe(tpy)_2]^{2+}$. The specific design of this non-permanent crosslinker allows preparing supramolecular hydrogels, using a one-step polymerization in water. The structure at a length scale higher than several tens of nanometers and the rheological behavior of the synthesized supramolecular gels were probed by light scattering and rheology experiments. Some similarities with PAM hydrogels crosslinked with MBA, at the same crosslinker feed ratio values, were observed. However, a study of the network structure as a function of the crosslinker feed ratio by ^{1}H DQ NMR points out some differences between chemical and supramolecular hydrogels, at the network chain length scale. Indeed, the supramolecular crosslinker seems to create a more homogeneous structure than the covalent one with less defects and a narrower distribution of the elastically effective strand size, up to a crosslinker feed ratio of 0.3 mol%. For a crosslinker content of 0.3 mol%, the supramolecular network structure gets as dense and polydisperse as the one of the chemical network, prepared with the same amount of MBA. In contrast, the chemical network only grows by replication of its structure in a self-similar way upon increasing the MBA feed ratio. These major differences between the Chem-PAM and Supra-PAM hydrogels do not seem to impact the elastic modulus of the supramolecular gels and might be explained by the presence of charges. The influence of these positive charges that result from the nature of the supramolecular

crosslinker is highlighted by the specific polyelectrolyte swelling behavior of the supramolecular gels, Supra-PAM, contrary to the neutral swelling behavior of the chemical gels, Chem-PAM. Another major difference between Supra-PAM and Chem-PAM gels stands in the crosslinker junction dynamics, since the supramolecular crosslinker is built from a non-permanent assembly. However, the lifetime of this complex is really long (10^7 s according to the literature) and as a result, the supramolecular crosslinks behave like covalent bonds over the observed timescales (up to 100 s).[9,55] Nevertheless, this non-permanent bond plays an important role as it can be activated on shorter timescales thanks to an oxidizing stimulus. A gradual transition from a gel to a polymer solution is induced by immersing the supramolecular gels into KPS solutions. The immersing time and the KPS content are as many experimental levers that can be used to finely modulate the physico-chemical properties of the supramolecular gels.

In summary, we developed a supramolecular crosslinker that allows a straightforward synthesis of a stimuli-responsive hydrogel with similar properties as a chemically-crosslinked gel, despite its different structure at the macromolecular length scale. However, one can expect differences in the non-linear domain in which the specific non-permanent nature of the supramolecular crosslinks might give rise to dissipation mechanisms. Moreover, in the non-linear domain, the differences in the network topology detected between both kinds of gels may play a role. Our promising system is also very versatile since it can be applied to other polymer systems. We are currently working on the copolymerization of this supramolecular crosslinker with stimuli-responsive monomers to build polymer networks that may undergo various transitions depending on the applied stimulus.

ASSOCIATED CONTENT

Supporting Information.

^{1}H NMR spectra, UV-vis spectroscopy, Rheology experiments

AUTHOR INFORMATION

Corresponding Authors

Patrick Perrin - Soft Matter Sciences and Engineering, ESPCI Paris, PSL University, Sorbonne University, CNRS, Paris Cedex 05, France.

Nicolas Sanson - Soft Matter Sciences and Engineering, ESPCI Paris, PSL University, Sorbonne University, CNRS, Paris Cedex 05, France.

Present Addresses

Sandrine Laquerbe - Soft Matter Sciences and Engineering, ESPCI Paris, PSL University, Sorbonne University, CNRS, Paris Cedex 05, France.

Julien Es Sayed - Soft Matter Sciences and Engineering, ESPCI Paris, PSL University, Sorbonne University, CNRS, Paris Cedex 05, France.

Cédric Lorthioir - Sorbonne Université, CNRS, Laboratoire de Chimie de la Matière Condensée de Paris, LCMCP, F-75005 Paris, France.

Christophe Meyer - Molecular, Macromolecular Chemistry, and Materials, (C3M)-UMR 7167 ESPCI Paris, PSL University, CNRS, Paris Cedex 05, France.

Tetsuharu Narita - Soft Matter Sciences and Engineering, ESPCI Paris, PSL University, Sorbonne University, CNRS, Paris Cedex 05, France.

Guylaine Ducouret - Soft Matter Sciences and Engineering, ESPCI Paris, PSL University, Sorbonne University, CNRS, Paris Cedex 05, France.

Author Contributions

The manuscript was written through contributions of all authors. All authors have given approval to the final version of the manuscript. Sandrine Laquerbe, Julien Es Sayed, Cédric Lorthioir, Christophe Meyer, Tetsuharu Narita, Guylaine Ducouret, Patrick Perrin and Nicolas Sanson contributed equally.

ACKNOWLEDGMENT

The authors gratefully acknowledge the financial support of CNRS, ESPCI, Sorbonne University and the PhD school of Sorbonne Université (ED 397, Sorbonne Université) for the PhD fellowship funding of S. Laquerbe. The solid-state NMR experiments were performed on a 300 MHz NMR spectrometer, the acquisition of which has been supported by the Region Ile-de-France in the framework of DIM Nano-K.

ABBREVIATIONS

Chem-PAM, chemically-crosslinked hydrogel; Supra-PAM, physically-crosslinked hydrogel; AM, acrylamide; PAM, polyacrylamide; NMR, nuclear magnetic resonance; DLS, dynamic light scattering; KCl, potassium chloride; KPS, potassium persulfate.

REFERENCES

(1) Caló, E.; Khutoryanskiy, V. V. Biomedical Applications of Hydrogels: A Review of Patents and Commercial Products. *Eur. Polym. J.* **2015**, *65*, 252–267. https://doi.org/10.1016/j.eurpolymj.2014.11.024.

(2) Hoare, T. R.; Kohane, D. S. Hydrogels in Drug Delivery: Progress and Challenges. *Polymer* **2008**, *49* (8), 1993–2007. https://doi.org/10.1016/j.polymer.2008.01.027.

(3) Rudzinski, W. E.; Dave, A. M.; Vaishnav, U. H.; Kumbar, S. G.; Kulkarni, A. R.; Aminabhavi, T. M. Hydrogels as Controlled Release Devices in Agriculture. *Des. Monomers Polym.* **2002**, *5* (1), 39–65. https://doi.org/10.1163/156855502760151580.

(4) Appel, E. A.; del Barrio, J.; Loh, X. J.; Scherman, O. A. Supramolecular Polymeric Hydrogels. *Chem. Soc. Rev.* **2012**, *41* (18), 6195. https://doi.org/10.1039/c2cs35264h.

(5) Webber, M. J.; Tibbitt, M. W. Dynamic and Reconfigurable Materials from Reversible Network Interactions. *Nat. Rev. Mater.* **2022**, *7* (7), 541–556. https://doi.org/10.1038/s41578-021-00412-x.

(6) Constable, E. The Coordination Chemistry of 2,2’-6’,2’’-Terpyridine And Higher Oligopyridines. *Adv. Inorg. Chem.* **1986**, *30*, 69–121. https://doi.org/10.1016/S0898-8838(08)60240-8.

(7) Chen, P.; Li, Q.; Grindy, S.; Holten-Andersen, N. White-Light-Emitting Lanthanide Metallogels with Tunable Luminescence and Reversible Stimuli-Responsive Properties. *J. Am. Chem. Soc.* **2015**, *137* (36), 11590–11593. https://doi.org/10.1021/jacs.5b07394.

(8) Andres, P. R.; Hofmeier, H.; Schubert, U. S. Complexation Parameters of Terpyridine-Metal Complexes. In *Metal-Containing and Metallosupramolecular Polymers and Materials*; ACS Symposium Series; American Chemical Society, 2006; Vol. 928, pp 141–156. https://doi.org/10.1021/bk-2006-0928.ch011.

(9) Hogg, R.; Wilkins, R. G. Exchanges Studies of Ceratin Chelate Compounds of Transitional Metals. Part VIII. 2,2’,2’’-Terpyridine Complexes. *J. Chem. Soc.* **1962**, No. JAN, 341-. https://doi.org/10.1039/jr9620000341.

(10) Potts, K. T.; Usifer, D. A. Polymers and Polymer-Metal Complexes Containing Pendent 2,2’:6’,2"-Terpyridinyl Ligands. *Macromolecules* **1988**, *21* (7), 1985–1991. https://doi.org/10.1021/ma00185a016.

(11) Hanabusa, K.; Nakamura, A.; Koyama, T.; Shirai, H. Synthesis, Polymerization, Copolymerization, and Transition-Metal Coordination of 4-(2,2′:6′,2″-Terpyridin-4′-Yl)Styrene and Its Polymers and Copolymers. *Makromol. Chem.* **1992**, *193* (6), 1309–1319. https://doi.org/10.1002/macp.1992.021930607.

(12) Shunmugam, R.; Gabriel, G. J.; Aamer, K. A.; Tew, G. N. Metal–Ligand-Containing Polymers: Terpyridine as the Supramolecular Unit. *Macromol. Rapid Commun.* **2010**, *31* (9–10), 784–793. https://doi.org/10.1002/marc.200900869.

(13) Lohmeijer, B. G. G.; Schubert, U. S. Playing LEGO with Macromolecules: Design, Synthesis, and Self-Organization with Metal Complexes. *J. Polym. Sci. Part Polym. Chem.* **2003**, *41* (10), 1413–1427. https://doi.org/10.1002/pola.10685.

(14) Calzia, K. J.; Tew, G. N. Methacrylate Polymers Containing Metal Binding Ligands for Use in Supramolecular Materials: Random Copolymers Containing Terpyridines. *Macromolecules* **2002**, *35* (16), 6090–6093. https://doi.org/10.1021/ma025551j.

(15) Hofmeier, H.; Schubert, U. S. Supramolecular Branching and Crosslinking of Terpyridine-Modified Copolymers: Complexation and Decomplexation Studies in Diluted Solution. *Macromol. Chem. Phys.* **2003**, *204* (11), 1391–1397. https://doi.org/10.1002/macp.200350003.

(16) Hackelbusch, S.; Rossow, T.; Becker, H.; Seiffert, S. Multiresponsive Polymer Hydrogels by Orthogonal Supramolecular Chain Cross-Linking. *Macromolecules* **2014**, *47* (12), 4028–4036. https://doi.org/10.1021/ma5008573.

(17) Zhang, X.; Yin, Y.; Yan, J.; Li, W.; Zhang, A. Thermo- and Redox-Responsive Dendronized Polymer Hydrogels. *Polym. Chem.* **2018**, *9* (6), 712–721. https://doi.org/10.1039/C7PY01284E.

(18) Fadeev, M.; Davidson-Rozenfeld, G.; Biniuri, Y.; Yakobi, R.; Cazelles, R.; Aleman-Garcia, M. A.; Willner, I. Redox-Triggered Hydrogels Revealing Switchable Stiffness Properties and Shape-Memory Functions. *Polym. Chem.* **2018**, *9* (21), 2905–2912. https://doi.org/10.1039/C8PY00515J.

(19) Brassinne, J.; Jochum, F.; Fustin, C.-A.; Gohy, J.-F. Revealing the Supramolecular Nature of Side-Chain Terpyridine-Functionalized Polymer Networks. *Int. J. Mol. Sci.* **2015**, *16* (1), 990–1007. https://doi.org/10.3390/ijms16010990.

(20) Xu, X.; Jerca, F. A.; Jerca, V. V.; Hoogenboom, R. Covalent Poly(2-Isopropenyl-2-Oxazoline) Hydrogels with Ultrahigh Mechanical Strength and Toughness through Secondary Terpyridine Metal-Coordination Crosslinks. *Adv. Funct. Mater.* **2019**, *29* (48), 1904886. https://doi.org/10.1002/adfm.201904886.

(21) Asoh, T.-A.; Yoshitake, H.; Takano, Y.; Kikuchi, A. Fabrication of Self-Healable Hydrogels through Sol–Gel Transition in Metallo-Supramolecular Aqueous Solution by Aeration. *Macromol. Chem. Phys.* **2013**, *214* (22), 2534–2539. https://doi.org/10.1002/macp.201300458.

(22) Ahmadi, M.; Löser, L.; Fischer, K.; Saalwächter, K.; Seiffert, S. Connectivity Defects and Collective Assemblies in Model Metallo-Supramolecular Dual-Network Hydrogels. *Macromol. Chem. Phys.* **2020**, *221* (1), 1900400. https://doi.org/10.1002/macp.201900400.

(23) Rossow, T.; Seiffert, S. Supramolecular Polymer Gels with Potential Model-Network Structure. *Polym. Chem.* **2014**, *5* (8), 3018–3029. https://doi.org/10.1039/C3PY01692G.

(24) Czarnecki, S.; Rossow, T.; Seiffert, S. Hybrid Polymer-Network Hydrogels with Tunable Mechanical Response. *Polymers* **2016**, *8* (3), 82. https://doi.org/10.3390/polym8030082.

(25) Zhu, C. N.; Bai, T.; Wang, H.; Bai, W.; Ling, J.; Sun, J. Z.; Huang, F.; Wu, Z. L.; Zheng, Q. Single Chromophore-Based White-Light-Emitting Hydrogel with Tunable Fluorescence and Patternability. *ACS Appl. Mater. Interfaces* **2018**, *10* (45), 39343–39352. https://doi.org/10.1021/acsami.8b12619.

(26) Candau, F.; Regalado, E. J.; Selb, J. Scaling Behavior of the Zero Shear Viscosity of Hydrophobically Modified Poly(Acrylamide)s. *Macromolecules* **1998**, *31* (16), 5550–5552. https://doi.org/10.1021/ma9802982.

(27) Es Sayed, J.; Meyer, C.; Sanson, N.; Perrin, P. Oxidation-Responsive Emulsions Stabilized by Cleavable Metallo-Supramolecular Cross-Linked Microgels. *ACS Macro Lett.* **2020**, *9* (7), 1040–1045. https://doi.org/10.1021/acsmacrolett.0c00389.

(28) Baum, J.; Pines, A. NMR Studies of Clustering in Solids. *J. Am. Chem. Soc.* **1986**, *108* (24), 7447–7454. https://doi.org/10.1021/ja00284a001.

(29) Saalwachter, K. Proton Multiple-Quantum NMR for the Study of Chain Dynamics and Structural Constraints in Polymeric Soft Materials. *Prog. Nucl. Magn. Reson. Spectrosc.* **2007**, *51* (1), 1–35. https://doi.org/10.1016/j.pnmrs.2007.01.001.

(30) Chassé, W.; Valentín, J. L.; Genesky, G. D.; Cohen, C.; Saalwächter, K. Precise Dipolar Coupling Constant Distribution Analysis in Proton Multiple-Quantum NMR of Elastomers. *J. Chem. Phys.* **2011**, *134* (4), 044907. https://doi.org/10.1063/1.3534856.

(31) Joosten, J. G. H.; McCarthy, J. L.; Pusey, P. N. Dynamic and Static Light Scattering by Aqueous Polyacrylamide Gels. *Macromolecules* **1991**, *24* (25), 6690–6699. https://doi.org/10.1021/ma00025a021.

(32) Wang, R.; Both, S. K.; Geven, M.; Calucci, L.; Forte, C.; Dijkstra, P. J.; Karperien, M. Kinetically Stable Metal Ligand Charge Transfer Complexes as Crosslinks in Nanogels/Hydrogels: Physical Properties and Cytotoxicity. *Acta Biomater.* **2015**, *26*, 136–144. https://doi.org/10.1016/j.actbio.2015.08.019.

(33) Metallo-Supramolecular Terpyridine Architectures. In *Modern Terpyridine Chemistry*; 2006; pp 69–130. https://doi.org/10.1002/3527608486.ch4.

(34) Rubinstein, M.; Colby, R. H. *Polymer Physics*; Oxford University Press, 2003.

(35) Calvet, D.; Wong, J. Y.; Giasson, S. Rheological Monitoring of Polyacrylamide Gelation: Importance of Cross-Link Density and Temperature. *Macromolecules* **2004**, *37* (20), 7762–7771. https://doi.org/10.1021/ma049072r.

(36) Adibnia, V.; Hill, R. J. Universal Aspects of Hydrogel Gelation Kinetics, Percolation and Viscoelasticity from PA-Hydrogel Rheology. *J. Rheol.* **2016**, *60* (4), 541–548. https://doi.org/10.1122/1.4948428.

(37) Orakdogen, N.; Okay, O. Correlation between Crosslinking Efficiency and Spatial Inhomogeneity in Poly(Acrylamide) Hydrogels. *Polym. Bull.* **2006**, *57* (5), 631–641. https://doi.org/10.1007/s00289-006-0624-1.

(38) Weiss, N.; Silberberg, A. Inhomogeneity of Polyacrylamide Gel Structure from Permeability and Viscoelasticity. *Br. Polym. J.* **1977**, *9* (2), 144–150. https://doi.org/10.1002/pi.4980090210.

(39) Baselga, J.; Llorente, M. A.; Nieto, J. L.; Hernández-Fuentes, I.; Piérola, I. F. Polyacrylamide Networks. Sequence Distribution of Crosslinker. *Eur. Polym. J.* **1988**, *24* (2), 161–165. https://doi.org/10.1016/0014-3057(88)90145-0.

(40) Gombert, Y.; Roncoroni, F.; Sánchez-Ferrer, A.; Spencer, N. D. The Hierarchical Bulk Molecular Structure of Poly(Acrylamide) Hydrogels: Beyond the Fishing Net. *Soft Matter* **2020**, *16* (42), 9789–9798. https://doi.org/10.1039/D0SM01536A.

(41) Yang, C.; Yin, T.; Suo, Z. Polyacrylamide Hydrogels. I. Network Imperfection. *J. Mech. Phys. Solids* **2019**, *131*, 43–55. https://doi.org/10.1016/j.jmps.2019.06.018.

(42) Zou, X.; Kui, X.; Zhang, R.; Zhang, Y.; Wang, X.; Wu, Q.; Chen, T.; Sun, P. Viscoelasticity and Structures in Chemically and Physically Dual-Cross-Linked Hydrogels: Insights from Rheology and Proton Multiple-Quantum NMR Spectroscopy. *Macromolecules* **2017**, *50* (23), 9340–9352. https://doi.org/10.1021/acs.macromol.7b01854.

(43) Du, C.; Hill, R. J. Linear Viscoelasticity of Weakly Cross-Linked Hydrogels. *J. Rheol.* **2019**, *63* (1), 109–124. https://doi.org/10.1122/1.5052160.

(44) Seiffert, S.; Sprakel, J. Physical Chemistry of Supramolecular Polymer Networks. *Chem Soc Rev* **2012**, *41* (2), 909–930. https://doi.org/10.1039/C1CS15191F.

(45) Shibayama, M.; Norisuye, T. Gel Formation Analyses by Dynamic Light Scattering. *Bull. Chem. Soc. Jpn.* **2002**, *75* (4), 641–659. https://doi.org/10.1246/bcsj.75.641.

(46) Ozaki, H.; Indei, T.; Koga, T.; Narita, T. Physical Gelation of Supramolecular Hydrogels Cross-Linked by Metal-Ligand Interactions: Dynamic Light Scattering and Microrheological Studies. *Polymer* **2017**, *128*, 363–372. https://doi.org/10.1016/j.polymer.2017.01.077.

(47) Henderson, I. M.; Hayward, R. C. Kinetic Stabilities of Bis-Terpyridine Complexes with Iron(Ii) and Cobalt(Ii) in Organic Solvent Environments. *J. Mater. Chem.* **2012**, *22* (40), 21366. https://doi.org/10.1039/c2jm33870j.

(48) Hooper, H. H.; Baker, J. P.; Blanch, H. W.; Prausnitz, J. M. Swelling Equilibria for Positively Ionized Polyacrylamide Hydrogels. *Macromolecules* **1990**, *23* (4), 1096–1104. https://doi.org/10.1021/ma00206a031.

(49) Baselga, J.; Hernández-Fuentes, I.; Masegosa, R. M.; Llorente, M. A. Effect of Crosslinker on Swelling and Thermodynamic Properties of Polyacrylamide Gels. *Polym. J.* **1989**, *21* (6), 467–474. https://doi.org/10.1295/polymj.21.467.

(50) Baker, J. P.; Hong, L. H.; Blanch, H. W.; Prausnitz, J. M. Effect of Initial Total Monomer Concentration on the Swelling Behavior of Cationic Acrylamide-Based Hydrogels. *Macromolecules* **1994**, *27* (6), 1446–1454. https://doi.org/10.1021/ma00084a026.

(51) Flory, P. J.; Rehner, J. Statistical Mechanics of Cross- Linked Polymer Networks II. Swelling. *J. Chem. Phys.* **1943**, *11* (11), 521–526. https://doi.org/10.1063/1.1723792.

(52) Yang, H.; Ghiassinejad, S.; van Ruymbeke, E.; Fustin, C.-A. Tunable Interpenetrating Polymer Network Hydrogels Based on Dynamic Covalent Bonds and Metal–Ligand Bonds. *Macromolecules* **2020**, *53* (16), 6956–6967. https://doi.org/10.1021/acs.macromol.0c00494.

(53) Es Sayed, J.; Lorthioir, C.; Banet, P.; Perrin, P.; Sanson, N. Reversible Assembly of Microgels by Metallo- Supramolecular Chemistry. *Angew. Chem. Int. Ed.* **2020**, *59* (18), 7042–7048. https://doi.org/10.1002/anie.201915737.

(54) Zhou, H.; Yang, Y.; Xu, G.; Chen, W.; Zhang, W.; Wang, Q.; Zheng, Z.; Ding, X. Ru(II)(Tpy)2-Functionalized Hydrogels: Synthesis, Reversible Responsiveness, and Coupling with the Belousov-Zhabotinsky Reaction. *J. Polym. Sci. Part Polym. Chem.* **2015**, *53* (19), 2214–2222. https://doi.org/10.1002/pola.27690.

(55) Henderson, I. M.; Hayward, R. C. Kinetic Stabilities of Bis-Terpyridine Complexes with Iron(Ii) and Cobalt(Ii) in Organic Solvent Environments. *J. Mater. Chem.* **2012**, *22* (40), 21366. https://doi.org/10.1039/c2jm33870j.